HHS Public Access

Author manuscript

Bioorg Med Chem Lett. Author manuscript; available in PMC 2015 May 11.

Published in final edited form as:

Bioorg Med Chem Lett. 2014 September 1; 24(17): 4158–4161. doi:10.1016/j.bmcl.2014.07.049.

Structural studies provide clues for analog design of specific inhibitors of *Cryptosporidium hominis* Thymidylate Synthase-Dihydrofolate Reductase

Vidya P. Kumar[a], **Jose A. Cisneros**[b], **Kathleen M. Frey**[a], **Alejandro Castellanos-Gonzalez**[c], **Yiqiang Wang**[d], **Aleem Gangjee**[d,*], **A. Clinton White Jr**[c], **William L. Jorgensen**[b,*], and **Karen S. Anderson**[a,*]

[a]Department of Pharmacology, Yale University School of Medicine, 333 Cedar Street, New Haven, CT 06520, USA

[b]Department of Chemistry, Yale University, 225 Prospect Street, PO Box 208107, New Haven, CT 06520-8107, USA

[c]Infectious Disease Division, Department of Internal Medicine, University of Texas Medical Branch, Galveston, USA

[d]Division of Medicinal Chemistry, Graduate School of Pharmaceutical Sciences, Duquesne University, Pittsburgh, PA 15282, USA

Abstract

Cryptosporidium is the causative agent of a gastrointestinal disease, cryptosporidiosis, which is often fatal in immunocompromised individuals and children. Thymidylate synthase (TS) and dihydrofolate reductase (DHFR) are essential enzymes in the folate biosynthesis pathway and are well established as drug targets in cancer, bacterial infections, and malaria. *Cryptosporidium hominis* has a bifunctional thymidylate synthase and dihydrofolate reductase enzyme, compared to separate enzymes in the host. We evaluated lead compound **1** from a novel series of antifolates, 2-amino-4-oxo-5-substituted pyrrolo[2,3-*d*]pyrimidines as an inhibitor of *Cryptosporidium hominis* thymidylate synthase with selectivity over the human enzyme. Complementing the enzyme inhibition compound **1** also has anti-cryptosporidial activity in cell culture. A crystal structure with compound **1** bound to the TS active site is discussed in terms of several van der Waals, hydrophobic and hydrogen bond interactions with the protein residues and the substrate analog 5-fluorodeoxyuridine monophosphate (TS), cofactor NADPH and inhibitor methotrexate (DHFR). Another crystal structure in complex with compound **1** bound in both the TS and DHFR active sites is also reported here. The crystal structures provide clues for analog design and for the design of *Ch*TS-DHFR specific inhibitors.

[*]Corresponding authors. Tel. +1 203 785 4526, fax. +1 203 785 7670 (KSA); Tel. +1 203 432 6278, fax. +1 203 432 6299 (WLJ); Tel: +1 412 396 6070, fax: +1 412 396 5593 (AG). karen.anderson@yale.edu; william.jorgensen@yale.edu; gangjee@duq.edu.

Supplementary data

Full details on the enzyme assays, crystallography, experimental section, synthesis of compound **1** is provided. This material is available free of charge via the Internet at http://www.elsevier.com. Data for compound **1** have been deposited in the RCSB Protein Data Bank with codes 4Q0D and 4Q0E.

Keywords

Thymidylate synthase; Cryptosporidium; Inhibitor; Dihydrofolate reductase; Crystal structure

Cryptosporidiosis, a protozoan gastrointestinal infection, continues to be a major reason for morbidity and mortality in immunocompromised individuals and young children[1]. Recent reports from the CDC estimate approximately 750,000 cases of cryptosporidiosis in United States each year[2-4]. *Cryptosporidium* is one of the four pathogens that cause most cases of moderate-to-severe diarrhea in infants and children in developing countries and was second to rotavirus as a cause of diarrheal morbidity and mortality in infants. Lack of effective treatment against cryptosporidiosis in immunocompromised individuals[4-6] raises the need for development of effective yet less toxic drugs. Information from the crystal structure along with computational studies could guide the design and development of parasite specific inhibitors.

Thymidylate synthase (TS) and dihydrofolate reductase (DHFR) are essential enzymes in the folate biosynthesis pathway and are well established as drug targets in cancer, bacterial infections, and malaria. In *Cryptosporidium hominis*, TS and DHFR exist as a bifunctional enzyme. In human, these enzymes are on two separate polypeptide chains. In the presence of the cofactor 5,10-methylene tetrahydrofolate (CH_2H_4F), TS catalyzes reductive methylation of deoxyuridine monophosphate (dUMP) to form deoxythymine monophosphate (dTMP) and dihydrofolate (H_2F). Dihydrofolate is then reduced to tetrahydrofolate in presence of NADPH by DHFR. In this study we report the x-ray crystal structures of *Cryptosporidium hominis* TS-DHFR (*Ch*TS-DHFR) in complex with compound **1** (Scheme 1), an antifolate from a novel series of 2-amino-4-oxo-5-substituted pyrrolo[2,3-*d*]pyrimidines. In the first crystal structure, compound **1** is bound to the TS active site in the presence of 5-fluorodeoxyuridine monophosphate (FdUMP, a TS substrate analog) whereas methotrexate (MTX, a folate analog) and NADPH (DHFR cofactor) to the DHFR site. The second crystal structure reveals that compound **1** binds to both TS and DHFR active sites in the presence of FdUMP (a TS substrate analog) and NADPH (DHFR cofactor). Analysis of the interactions between the inhibitor, cofactors and the active site residues can be utilized to design parasite specific inhibitors.

Previous studies have evaluated compound **1** (2-amino-4-oxo-4,7-dihydro-pyrrolo[2,3-*d*]pyrimidine-methyl-phenyl-*L*-glutamic acid) on human and cryptosporidial forms of TS (hTS)[7] and C*h*TS-DHFR[8]. In this study we evaluate its effect on *Ch*TS-DHFR while comparing its activity on the human enzymes in combination with structural studies. While the synthesis of compound **1** has been reported earlier[7, 9], a modified synthetic route (Scheme 1) is shown below that offers improvements in terms of more readily accessible precursors and shorter reaction times.

When tested against *Ch*TS enzyme activity, compound **1** was found to be more potent on the parasite enzyme in comparison with the human enzyme. The *Ch*TS catalytic activity was inhibited with an IC_{50} value of 0.38 ± 0.04 μM with a 5-fold selectivity with respect to hTS (IC_{50} value of 1.80 ± 0.45 μM). Compound **1** also inhibited DHFR enzyme activity with

IC_{50} values of 0.049 ± 0.005 μM for *Ch*DHFR and 0.64 ± 0.04 μM for hDHFR, respectively.

In this study, we also evaluated the anti-cryptosporidial activity of compound **1** on *Cryptosporidium parvum* sporozoites and in intracellular forms of the parasite in cell culture. Compound **1** significantly reduced parasite infection in cell culture, with a half maximal effective concentration ranging from 1 – 5 μM (Figure S5). Microscopically there were no morphological differences in treated and untreated cells. The ratios of dead and alive cells and ribosomal RNA levels in the treated and untreated cells were similar (data not shown). The detailed procedure for the cell culture assay is provided in the Supplementary data.

In an attempt to co-crystallize *Ch*TS-DHFR with compound **1**, multiple combinations of TS and DHFR site ligands were examined. Co-crystallization with compound **1** and FdUMP in the TS site and NADPH and MTX in DHFR site resulted in a crystal structure of 3.45 Å (Figure S1A, PDB code 4Q0D). Compound **1** bound to both the TS and DHFR active sites along with FdUMP and NADPH to yield a higher resolution (2.7 Å) structure (Figure S1B, PDB code 4Q0E). Detailed crystallization conditions are reported in the Supplementary data. The general *Ch*TS-DHFR structure bound to compound **1** is similar in both structures with a root mean square deviation (RMSD) of 0.54 (Figure S2). In both structures, all residues from 3 to 521 except for residues 179 – 192 are clearly defined in the electron density, allowing all of the ligand binding sites of the structure to be visualized. When compound **1** is bound to the TS active site, the structure is essentially similar whether compound **1** or MTX is bound at the DHFR active site. Here we report both crystal structures as the higher resolution structure with compound **1** bound to both active sites allowed a more detailed analysis of important inhibitor-protein interactions.

Figure 1 shows $2mF_o$-F_c electron density maps of the active site region of *Ch*TS bound to compound **1** revealing the positions of the FdUMP and compound **1** complex. Omit σ_A-weighted $2mF_o$-F_c electron density maps and data collection and refinement statistics are reported in the Supplementary data (Figure S3). The TS active site predominantly consists of hydrophobic residues, N256, A287, I315, W316, L399, F433, and M519 in addition to D518. At the TS site, compound **1** binds close to FdUMP, the pyrrolo[2,3-*d*]pyrimidine scaffold of compound **1** stacking with the pyrimidine ring of FdUMP. Several hydrophobic and van der Waals interactions are seen between compound **1** and L399, W316 and Y466 (Figure 2). The phenyl ring of compound **1** interacts with residues I315, F433 and M519. The non-conserved and unique residue A287 interacts with the glutamate tail of the inhibitor[10]. Four hydrogen bonds stabilize compound **1** optimally in the TS active site. The carbonyl O of D426 hydrogen bonds with N3 and the carbonyl O of N319 with N7 and the amino group of G430 hydrogen bonds with 4-oxo group of compound **1**. The 2-amino group of compound **1** hydrogen bonds with the hydroxyl group of Y466 and carbonyl O of A520.

Compound **1** has several hydrogen bonds and van der Waals interactions with the DHFR active site residues, binding close to the nicotinamide ring of NADPH (Figure S4). NADPH binds in an extended form making several hydrophobic and hydrogen bond interactions with the protein residues. The hydrophobic pocket consists of V9, A11, L25, I62 and T134

interacting with the pyrrolo[2,3-*d*]pyrimidine scaffold whereas T40 and F36 interact with the phenyl ring of compound **1**. The carbonyl oxygens of the catalytic D32 hydrogen bond with N3 of compound **1** forming a fork that holds the inhibitor in optimal position, as seen in the case of H_2F in *Ch*TS-DHFR:H_2F complex[11]. The amino group of V10 hydrogen bonds with N1 of compound **1** while the carboxyl of V9 interacts with N7 of compound **1**. The N7 of compound **1** also interacts with the unique residue C113. The flexible glutamate tail of compound **1** is held in place by four hydrogen bonds to R70, S37 and K34. Though compound **1** binds to TS and DHFR active sites, the interactions and the conformation of the inhibitor in two sites is distinct in each case.

In summary, we report compound **1** (2-amino-4-oxo-4,7-dihydro-pyrrolo[2,3-*d*]pyrimidine-methyl-phenyl-*L*-glutamic acid) as a potent inhibitor of *Ch*TS with anti-cryptosporidial activity is cell culture. Though most residues in *Ch*TS active site are conserved, there are two residues (A287 and S290) which are unique to *Ch*TS. In other parasite species and also human, these residues are Phe and Gly, respectively[12, 13]. These residues have been shown to be important for optimal positioning of the cofactor CH_2H_4F and catalysis[10]. In addition to the van der Waals interaction between the glutamate tail of compound **1** and A287, the structural differences between *Ch*TS and hTS can be exploited to design a parasite specific TS inhibitor. The strategy is to focus on improving the selectivity against human enzyme without compromising the activity against *Ch*TS-DHFR by using the newly solved crystal structure coupled with computer-aided design. This strategy is greatly facilitated by the structural information of the complex with the lead compound **1**, presented here. Promising anti-cryptosporidial activity was observed in parasite infected cells, although delivery of the compound through the parasitophorous vacuolar membranes requires new drug delivery strategies that are currently being explored in order to have better potency towards the intracellular parasites.

Supplementary Material

Refer to Web version on PubMed Central for supplementary material.

Acknowledgment

This work is supported by NIAID grant (AI083146) to KSA, NIAID grant (AI104334) to KMF, the Paul R Stalnaker MD Distinguished Professorship to ACW, NCI grant (CA152316) and the Duquesne University Adrian Van Kaam Chair in Scholarly Excellence to AG and NIH grant (GM32136) to WLJ.

References

1. Kotloff KL, Nataro JP, Blackwelder WC, Nasrin D, Farag TH, Panchalingam S, Wu Y, Sow SO, Sur D, Breiman RF, Faruque AS, Zaidi AK, Saha D, Alonso PL, Tamboura B, Sanogo D, Onwuchekwa U, Manna B, Ramamurthy T, Kanungo S, Ochieng JB, Omore R, Oundo JO, Hossain A, Das SK, Ahmed S, Qureshi S, Quadri F, Adegbola RA, Antonio M, Hossain MJ, Akinsola A, Mandomando I, Nhampossa T, Acácio S, Biswas K, O'Reilly CE, Mintz ED, Berkeley LY, Muhsen K, Sommerfelt H, Robins-Browne RM, Levine MM. Lancet. 2013; 382:209. [PubMed: 23680352]
2. Feng Y, Tiao N, Li N, Hlavsa M, Xiao L. J Clin Microbiol. 2013
3. Scallan E, Hoekstra RM, Angulo FJ, Tauxe RV, Widdowson MA, Roy SL, Jones JL, Griffin PM. Emerg Infect Dis. 2011; 17:7. [PubMed: 21192848]

4. Checkley W, White AC Jr. Jaganath D, Arrowood MJ, Chalmers RM, Chen X-M, Fayer R, Griffiths JK, Guerrant RL, Hedstrom L, Huston CD, Kotloff KL, Kang G, Mead JR, Miller M, Petri W Jr. Priest JW, Roos DS, Striepen B, Thompson RA, Ward HD, Van Voorhis WC, Xiao L, Zhu G, Houpt ER. Lancet Infect Dis. 2014
5. Abubakar I, Aliyu SH, Arumugam C, Usman NK, Hunter PR. Br J Clin Pharmacol. 2007; 63:387. [PubMed: 17335543]
6. Gargala G, Delaunaya A, Lib X, Brasseurb P, Favennecb L, Balleta JJ. J Antimicrob Chemother. 2000; 46:57. [PubMed: 10882689]
7. Aso K, Imai Y, Yukishige K, Ootsu K, Akimoto H. Chem. Pharm. Bull. 2001; 49:1280. [PubMed: 11605654]
8. Kumar VP, Frey KM, Wang Y, Jain HK, Gangjee A, Anderson KS. Bioorganic & medicinal chemistry letters. 2013; 23:5426. [PubMed: 23927969]
9. Wang YR,S, Ravindra MP, Hales E, Orr S, Cherian C, Hou Z, Matherly LH, Gangjee A. J. Med. Chem. 2013; 56:10016. [PubMed: 24256410]
10. Doan LT, Martucci WE, Vargo MA, Atreya CE, Anderson KS. Biochemistry. 2007; 46:8379. [PubMed: 17580969]
11. Anderson AC. Acta Crystallogr Sect F Struct Biol Cryst Commun. 2005; 61:258.
12. Martucci WE, Vargo MA, Anderson KS. Biochemistry. 2008; 47:8902. [PubMed: 18672899]
13. Vásquez JR, Goozé L, Kim K, Gut J, Petersen C, Nelson RG. Mol Biochem Parasitol. 1996; 79:153. [PubMed: 8855552]

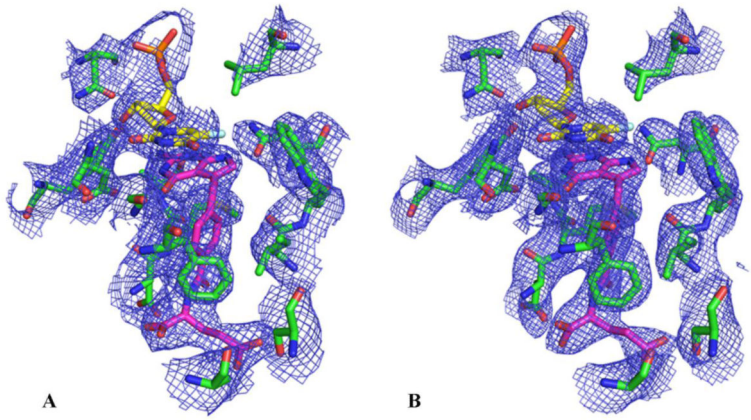

Figure 1.

$2mF_o$-F_c election density maps for TS active site of *Ch*TS-DHFR: FdUMP: compound **1** complex (A) with MTX and NADPH in the DHFR site (contour level at 1.0 σ) (B) with compound **1** and NADPH in the DHFR site (contour level at 1.3 σ).

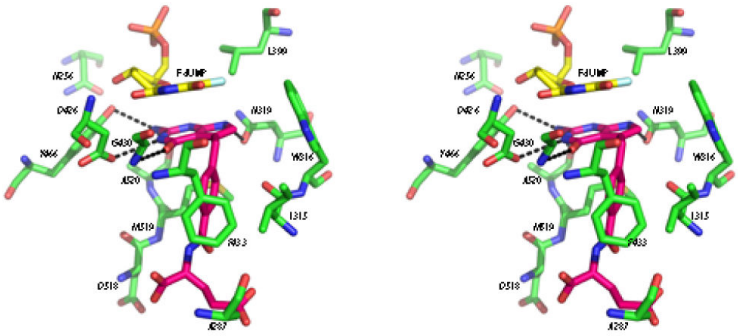

Figure 2.

Stereo view of active site residues of *Ch*TS (green) interacting with FdUMP (yellow) and compound **1** (pink). Hydrogen bonds (< 3.5 Å) are indicated as dashed lines.

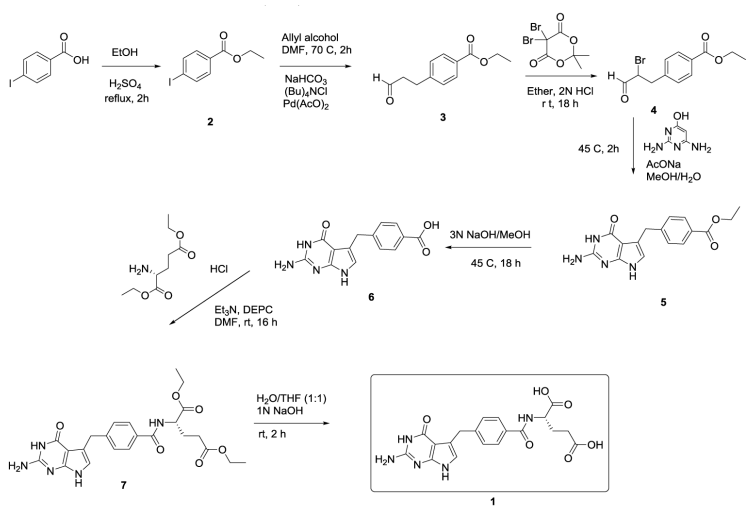

Scheme 1.
Synthesis of compound 1.